Inorganica Chimica Acta 374 (2011) 572–577

Contents lists available at ScienceDirect

Inorganica Chimica Acta

journal homepage: www.elsevier.com/locate/ica

Cationic palladium(II) complexes of the sterically hindered bis(4-methylthiazolyl)isoindoline (4-Mebti) with neutral group XVI donor ligands

Martin Bröring *, Christian Kleeberg, Anne Scheja

Technische Universität Braunschweig, Institut für Anorganische und Analytische Chemie, Hagenring 30, 38106 Braunschweig, Germany

ARTICLE INFO

Article history:
Available online 13 March 2011

Dedicated to Prof. Dr. Wolfgang Kaim on the occasion of his 60th birthday.

Keywords:
BAI ligands
Palladium
Cationic complexes
Group 16 donors
X-ray structure determination

ABSTRACT

A series of cationic palladium complexes $[(4\text{-Mebti})PdL]^+$ with 4-Mebti = anion of bis(4-methylthiazolylimino)isoindoline and L = neutral ligand with group 16 donor atom has been prepared from the chlorido derivative [(4-Mebti)PdCl] and $NaBAr^F$ (BAr^F = tetrakis(3,5-bis(trifluoromethyl)phenyl)boranate) in the presence of the respective donor ligand. Crystallographic and spectroscopic analyses were achieved for species with L = SMe_2, $SeMe_2$, dmf, acetamide, diphenylurea, and formiate. The latter two complexes represent products from hydrolyses of phenyl isocyanate and dmf, respectively, which occur during the ligand exchange reactions. Several other O-donor ligands like thf, acetone, Me_2O, water, and others are not bound to the palladium ion, and the dinuclear μ-chlorido derivative $[\{(4\text{-Mebti})Pd\}_2Cl]^+$ is isolated in these cases instead. The crystallographic analyses prove the expected presence of distorted, pseudo-planar palladium chelates, and the degree of distortion correlates well with the chemical shifts observed for the proton nuclei of the terminal methyl groups in the ^1H NMR experiment.

1. Introduction

Ligand exchange processes of square-planar palladium(II) compounds and other *low spin* d^8 complexes have always shown associative reaction mechanisms in the cases studied so far [1]. A general possibility to move this mechanism towards a dissociative process and to observe a rare three-coordinate, T-shaped palladium(II) compound would lie in the kinetic destabilization of the square-planar ligand sphere. Such a scenario can be realized by applying a suitably substituted meridional tridentate ligand to a palladium ion. α,ω-Dimethyltripyrrins provide for such a ligand class and have been studied by us in the past towards this goal [2–8]. In these ligands backbones, the terminal methyl groups are oriented in a way that the fourth coordination site of a central palladium atom may not be occupied in the N_3 plane of the cationic (trpy)Pd fragment without significant distortion of either the organic ligand or the coordination geometry. As illustrated in Fig. 1, either of two forms is usually observed, the pseudo-planar form and the helical form, depending on the shape and sterical requirement of the employed additional ligand. In some cases an equilibrium exists, and both forms are observed crystallographically [4,5].

In a foregoing study, we have used group 14 and 15 donor ligands (C, N, P) with a stepwise increase in steric hindrance in order to push a (trpy)PdL compound towards dissociation into the three-coordinate T-shaped 14 VE cation. This approach failed as the system accepts quite large distortions with these strongly binding ligands, and escapes in the case of PMe_3 towards a square–pyramidal five-coordinate 18 VE complex. Applying weaker ligands resulted in the decomposition of the sensitive tripyrrin scaffold [8]. We have now turned to the more robust and structurally related bis(4-methylthiazolylimino)isoindoline (4-Mebti) framework [9,10], and report here a series of cationic palladium complexes with group 16 donor ligands (O, S, Se).

2. Experimental

2.1. General remarks

Reagents were purchased from commercial sources and used without further purification. Solvents were dried by conventional methods and stored under Argon. The preparation of the cationic complexes was performed using standard Schlenk techniques. [(4-Mebti)PdCl] **1** [11], sodium tetrakis(3,5-bis(trifluoromethyl)phenyl)boranate ($NaBAr^F$ [12]), and dimethylselenium [13] were prepared according to the literature methods. NMR spectra were recorded on a Bruker Avance 300 or DRX 400 spectrometer, respectively. Chemical shifts (δ) are given in ppm, using the resonance of the residual solvent CD_2Cl_2 as internal reference (^1H NMR: 5.32 ppm, ^{13}C NMR: 53.5 ppm). Nomenclature and

* Corresponding author. Tel.: +49 (0) 531 391 5302; fax: +49 (0) 531 391 5387.
E-mail address: m.broering@tu-bs.de (M. Bröring).

0020-1693/$ - see front matter © 2011 Elsevier B.V. All rights reserved.
doi:10.1016/j.ica.2011.02.080

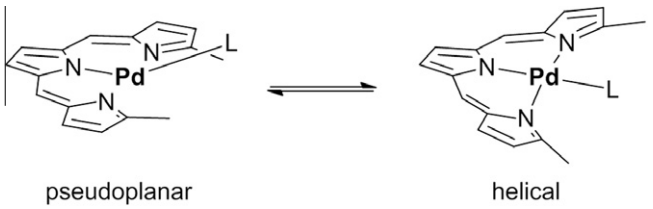

Fig. 1. Conformational dynamics observed for palladium complexes with sterically hindered tripyrrin ligands.

numbering scheme for the assignment of the resonance signals is given in Chart 1. In the case of ^{19}F NMR spectra, $CFCl_3$ was used as external reference. Elemental analyses were carried out on an Elementar Vario EL instrument. Melting points were determined on a Büchi SMP-20 in open capillaries and are not corrected.

2.2. Single crystal X-ray structural determinations

Experimental details relating to the crystallographic characterization are summarized in Table 1. Diffraction data were collected using graphite monochromated Mo Kα radiation on a Stoe IPDS-I instrument at 193(2) K using Φ-scans, or on a Stoe IPDS-II at 173(2) K using ω-scans. The structures were solved by direct methods and refined against F^2 by least-squares utilizing the software packages SHELXL-97 [14], SIR-92 [15], PLATON [16], and WINGX [17]. All non-hydrogen atoms were refined anisotropically. Hydrogen atoms were placed in calculated positions and refined using a riding model. Selected bond lengths, distances and angles for **2**–**7** are given in Table 2.

2.3. Syntheses of complexes

2.3.1. General procedure

[(4-Mebti)PdCl] **1** (10.0 mg, 21 μmol) was dissolved in dry toluene or dichloromethane (2 mL), and $NaBAr^F$ (18.7 mg, 21 μmol) was added in one portion. The mixture was stirred for 5 min before the neutral ligand was added, and stirring continued for 16 h. If a red solid has precipitated, the solvent was removed in vacuum and the solid extracted with dry dichloromethane. After filtration on celite the solvent was removed again, the residue washed with pentane, and dried in vacuum. If the product remained in solution, the reaction mixture was directly filtered and treated as described. Purification was achieved by crystallization as detailed below for each case.

2.3.2. [(4-Mebti)Pd(OC(NH$_2$)Me)]$^+$ BAr^{F-} (**2**)

Purified acetamide (5.9 mg, 100 μmol) and dichloromethane were used for the preparation. Single crystals of **2** were obtained after double recrystallization from toluene/*n*-pentane and dichloromethane/*n*-pentane, respectively. (14.6 mg, 51%), mp 168–170 °C ($C_{50}H_{29}BF_{24}N_6OPdS_2 \times CH_2Cl_2$ requires: C, 42.18; H, 2.15; N, 5.79. Found: C, 42.13; H, 2.57; N, 6.02%). ^1H NMR (CD_2Cl_2, 295 K): δ 2.02 (br s, 3H, acetamide), 2.57 (s, 6H, 4-Me_{Th}), 6.40–6.71 (br s, 2H, NH_2), 6.98 (s, 2H, 5-CH_{Th}), 7.56 (s, 4H, *p*-CH_{BAr^F}), 7.71–7.74 (m, 10H, β-CH + *o*-CH_{BAr^F}), 8.02–8.04 ppm (m, 2H, α-CH). ^{13}C NMR (CD_2Cl_2, 295 K): δ 19.3, 115.9, 117.9 (m, *p*-CH_{BAr^F}), 123.4, 125.0 (q, $^1J_{C-F}$ = 271 Hz, CF_3), 129.1 (m, *m*-C_{BAr^F}), 133.1, 135.2, 136.6, 150.2, 154.1, 162.0 (m, BC_{BAr^F}), 167.6 ppm; the remaining signal for the acetamide could not be detected. ^{19}F NMR (CD_2Cl_2, 295 K): δ −65.5 ppm.

2.3.3. [(4-Mebti)Pd(dmf)]$^+$ BAr^{F-} (**3**) and [(4-Mebti)Pd(OCHO)] (**4**)

A mixture of toluene and DMF (60:1) was used for the preparation. Single crystals of **3** were obtained by diffusion of *n*-pentane into a dichloromethane solution at −20 °C. (15.7 mg, 54%), mp 132 °C (decomp.) ($C_{51}H_{31}BF_{24}N_6OPdS_2$ requires: C, 44.36; H, 2.26; N, 6.08. Found: C, 43.92; H, 2.41; N, 5.99%). ^1H NMR (CD_2Cl_2, 295 K): δ 2.60 (s, 6H, 4-Me_{Th}), 2.98 (s, 3H, dmf), 3.01 (s, 3H, dmf), 6.91 (s, 2H, 5-CH_{Th}), 7.56 (s, 4H, *p*-CH_{BAr^F}), 7.66–7.69 (m, 2H, β-CH), 7.73 (br s, 8H, *o*-CH_{BAr^F}), 7.89–7.92 ppm (m, 2H, α-CH), 8.01 (s, 1H, dmf). ^{13}C NMR (CD_2Cl_2, 295 K): δ 19.7, 33.5, 38.2, 115.2, 117.4 (m, *p*-CH_{BAr^F}), 123.0, 124.7 (q, $^1J_{C-F}$ = 273 Hz, CF_3), 128.9 (m, *m*-C_{BAr^F}), 132.6, 134.7, 136.3, 149.5, 153.7, 161.9 (m, BC_{BAr^F}), 166.3, 166.8 ppm. ^{19}F NMR (CD_2Cl_2, 295 K): δ −62.9 ppm. If wet THF is added to the crystallization mixture, a small deposit of crystals of the formiate complex **4** forms over several days.

2.3.4. [(4-Mebti)Pd(OC(NHPh)$_2$)]$^+$ BAr^{F-} (**5**)

Wet toluene and phenylisocyanate (0.1 mL, 92 μmol) were used for the preparation. Single crystals of **5** were obtained by diffusion of *n*-pentane into a dichloromethane solution at −20 °C. (10.2 mg, 58%), mp 172 °C (decomp.) ($C_{61}H_{36}BF_{24}N_7OPdS_2$ requires: C, 48.19; H, 2.39; N, 6.45. Found: C, 47.47; H, 2.95; N, 7.27%). ^1H NMR (CD_2Cl_2, 295 K): δ 2.61 (s, 6H, 4-Me_{Th}), 6.84 (s, 2H, 5-CH_{Th}), 7.10–7.28 (m, 10H, CH_{Ph}), 7.56 (s, 4H, *p*-CH_{BAr^F}), 7.64 (s, 2H, β-CH), 7.73 (m, 10H, α-CH + *o*-CH_{BAr^F}); the NH signal was not detected. ^{13}C NMR (CD_2Cl_2, 295 K): δ 19.8, 115.0, 117.5 (m, *p*-CH_{BAr^F}), 122.9, 123.0, 124.7 (q, $^1J_{C-F}$ = 270 Hz, CF_3), 126.5, 129.0 (m, *m*-C_{BAr^F}), 129.8, 132.6, 134.9, 135.9, 136.2, 149.8, 153.4, 162.0 (m, BC_{BAr^F}), 166.2; the carbonyl carbon atom was not detected. ^{19}F NMR (CD_2Cl_2, 295 K): δ −65.4 ppm.

2.3.5. [(4-Mebti)Pd(SMe$_2$)]$^+$ BAr^{F-} (**6**)

A mixture of toluene and dimethylsulfide (25:1) was used for the preparation. Single crystals of **6** were obtained by diffusion of *n*-pentane into a dichloromethane solution at −20 °C. (18.7 mg, 65%), mp 163–166 °C ($C_{50}H_{30}BF_{24}N_5PdS_3 \times 1.86\ CH_2Cl_2$ (from the crystallographic analysis) requires: C, 40.59; H, 2.23; N, 4.57. Found: C, 40.62; H, 2.42; N, 4.44%). ^1H NMR (CD_2Cl_2, 295 K): δ 2.14 (s, 6H, Me_2S), 2.77 (s, 6H, 4-Me_{Th}), 7.13 (s, 2H, 5-CH_{Th}), 7.56 (br s, 4H, *p*-CH_{BAr^F}), 7.73 (br s, 8H, *o*-CH_{BAr^F}), 7.76 (m, 2H, β-CH),

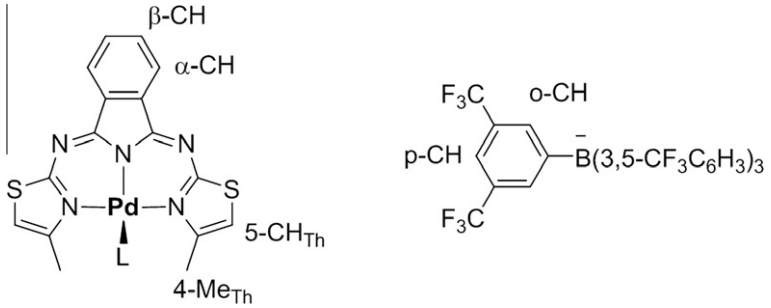

Chart 1. Nomenclature and numbering systems for the spectroscopic assignments.

Table 1
Crystallographic data and structure refinement parameters for **2–7**.

Compound	**2**	**3**	**4**	**5**	**6**	**7**
Formula	$C_{18}H_{17}N_6OPdS_2$, $C_{32}H_{12}BF_{24}$, CH_2Cl_2	$C_{19}H_{19}N_6OPdS_2$, $C_{32}H_{12}BF_{24}$	$C_{17}H_{13}N_5O_2PdS_2$,0.5 C_4H_8O	$C_{29}H_{24}N_7OS_2Pd$, $C_{32}H_{12}BF_{24}$	$C_{18}H_{18}N_5PdS_3$, $C_{32}H_{12}BF_{24}$, 1.86 CH_2Cl_2	$C_{18}H_{18}N_5PdS_2Se$, $C_{32}H_{12}BF_{24}$, 1.79 CH_2Cl_2
Formula weight	1452.09	1381.19	526.65	1520.34	1528.19	1569.24
Color/habit	orange/block	red/block	red/fragment	red/block	red/block	red/block
Crystal system	triclinic	triclinic	monoclinic	triclinic	monoclinic	monoclinic
Space group	$P\bar{1}$	$P\bar{1}$	$P2_1/n$	$P\bar{1}$	$P2_1/c$	$P2_1/c$
a (Å)	13.1121(7)	13.066(2)	8.8497(7)	13.940(2)	13.415(2)	13.373(1)
b (Å)	14.274(2)	13.811(4)	18.3119(9)	15.362(2)	22.188(2)	22.144(3)
c (Å)	16.714(2)	16.748(3)	12.3881(9)	17.416(2)	20.856(2)	20.873(2)
α (°)	75.31(1)	114.26(3)	90	105.19(1)	90	90
β (°)	82.31(2)	90.81(2)	100.267(6)	105.42(2)	103.78(1)	103.000(7)
γ (°)	68.98(2)	90.59(3)	90	90.25(2)	90	90
V (Å^3)	2821.3(7)	2755(1)	1975.4(2)	3458.8(8)	6029(1)	6023(1)
Z	2	2	4	2	4	4
D_c (g cm^{-3})	1.709	1.665	1.769	1.461	1.698	1.727
μ (mm^{-1})	0.622	0.540	1.181	0.439	0.702	1.25
F (0 0 0)	1440	1372	1058	1671	3401	3086
Crystal size (mm)	0.36 × 0.27 × 0.06	0.42 × 0.36 × 0.18	0.36 × 0.24 × 0.11	0.37 × 0.31 × 0.23	0.48 × 0.32 × 0.16	0.23 × 0.22 × 0.05
T (K)	193(2)	193(2)	100(2)	193(2)	193(2)	173(2)
θ-range (°)	1.86–26.14	2.07–26.02	2.01–25.41	1.97–26.01	1.81–26.11	1.81–26.04
Reflections collected	28 128	27 118	10 088	33 864	47 361	32 330
Reflections [$I > 2\sigma(I)$]	7679	7832	2573	8621	8634	6557
Data/restraints/parameters	10 369/6/852	9994/0/919	3585/35/292	12 560/46/959	11 785/15/939	11 724/5/824
Goodness-of-fit	0.980	0.946	0.956	0.955	1.048	0.923
Final R_1 [$I > 2\sigma(I)$]	0.0454	0.0393	0.0501	0.0529	0.0553	0.0605
Final wR_2 (all data)	0.1228	0.1038	0.1277	0.1453	0.1605	0.1320

Table 2
Selected bond lengths (Å) and bond angles (°) for the palladium complexes **2–7**.

	2 [D=O(1)]	**3** [D=O(1)]	**4** [D=O(2)]	**5** [D=O(1)]	**6** [D=S(3)]	**7** [D=Se(1)]
Pd–N(1)	2.033(3)	2.022(3)	2.026(5)	2.031(4)	2.030(4)	2.025(4)
Pd–N(3)	1.968(3)	1.968(2)	1.976(5)	1.962(3)	2.009(3)	2.010(4)
Pd–N(4)	2.038(3)	2.029(3)	2.041(5)	2.059(4)	2.017(4)	2.015(5)
Pd–D	2.068(3)	2.100(2)	2.026(4)	2.047(3)	2.357(1)	2.4650(8)
C(1)···C(16)	4.516(8)	4.374(6)	4.73(1)	4.788(8)	4.253(8)	4.35(1)
C(1)···D	2.838(6)	2.926(5)	2.770(9)	2.790(6)	3.240(7)	3.226(7)
C(16)···D	2.811(6)	2.921(5)	2.765(9)	2.776(6)	3.197(5)	3.283(9)
N(1)–Pd–N(3)	89.2(1)	90.4(1)	89.6(2)	89.9(2)	89.2(1)	89.1(2)
N(1)–Pd–N(5)	166.3(1)	169.59(9)	171.8(2)	170.4(1)	163.6(2)	164.9(2)
N(1)–Pd–D	93.7(1)	92.0(1)	90.2(2)	89.7(2)	95.6(1)	93.6(1)
N(3)–Pd–N(5)	89.7(1)	89.5(1)	90.2(2)	90.3(1)	88.6(1)	89.3(2)
N(3)–Pd–D	162.6(1)	156.30(9)	166.7(2)	166.2(1)	151.7(1)	150.8(1)
N(5)–Pd–D	91.4(1)	92.27(9)	91.9(2)	92.4(1)	94.0(1)	95.1(1)

8.08 (m, 2H, α-CH). ^{13}C NMR (CD_2Cl_2, 295 K): δ 19.9, 24.5, 116.4, 117.6 (m, p-CH_{BAr^F}), 123.4, 124.7 (q, $^1J_{C-F}$ = 271 Hz, CF_3), 129.0 (m, m-C_{BAr^F}), 133.2, 134.9, 136.6, 148.0, 155.2, 161.8 (m, BC_{BAr^F})), 167.9. ^{19}F NMR (CD_2Cl_2, 295 K): δ −62.8 ppm.

*2.3.6. [(4-Mebti)Pd(SeMe$_2$)]$^+$ BAr^{F-} (**7**)*

Toluene and dimethylselenide (1.7 μL, 22 μmol) was used for the preparation. Single crystals of **7** were obtained by diffusion of *n*-pentane into a dichloromethane solution at −20 °C. (20.2 mg, 68%), mp 155 °C (decomp.) ($C_{50}H_{30}BF_{24}N_5PdS_2Se$ requires: C, 42.38; H, 2.13; N, 4.94. Found: C, 42.06; H, 2.52; N, 4.58%). ^{1}H NMR (CD_2Cl_2, 295 K): δ 2.04 (s, 6H, Me_2S), 2.76 (s, 6H, 4-Me_{Th}), 7.11 (s, 2H, 5-CH_{Th}), 7.57 (br s, 4H, p-CH_{BAr^F}), 7.75 (br s, 8H, β-CH + o-CH_{BAr^F}), 8.07 (m, 2H, α-CH). ^{13}C NMR (CD_2Cl_2, 295 K): δ 15.6, 20.7, 116.2, 117.6 (m, p-CH_{BAr^F}), 123.3, 125.1 (q, $^1J_{C-F}$ = 270 Hz, CF_3), 129.3 (m, m-C_{BAr^F}), 133.1, 134.9, 136.7, 148.1, 156.3, 162.0 (m, BC_{BAr^F}), 167.9. ^{19}F NMR (CD_2Cl_2, 295 K): δ −64.4 ppm.

3. Results and discussion

3.1. Preparation of complexes

Cationic palladium(II) complexes with the 4-Mebti ligand can be prepared successfully by salt metathesis of the chlorido derivative [(4-Mebti)PdCl] **1** with sodium tetrakis(3,5-bis(trifluoromethyl)phenyl)boranate (NaBAr^F) [12] in the presence of different neutral ligands and solvents. The use of the chlorido precursor **1** is recommended over the analogous and more accessible acetato derivative [18] as the low solubility of sodium chloride appears to be the major driving force for the reaction with neutral donor ligands. A similar approach has successfully been applied for a number of cationic palladium(II) precatalysts for norbornene polymerization [19,20]. Scheme 1 presents an overview of successful preparations and of unsuccessful attempts.

The outcome of the attempted ligand exchange reactions can be divided into three classes. Hard O-donor ligands of the group

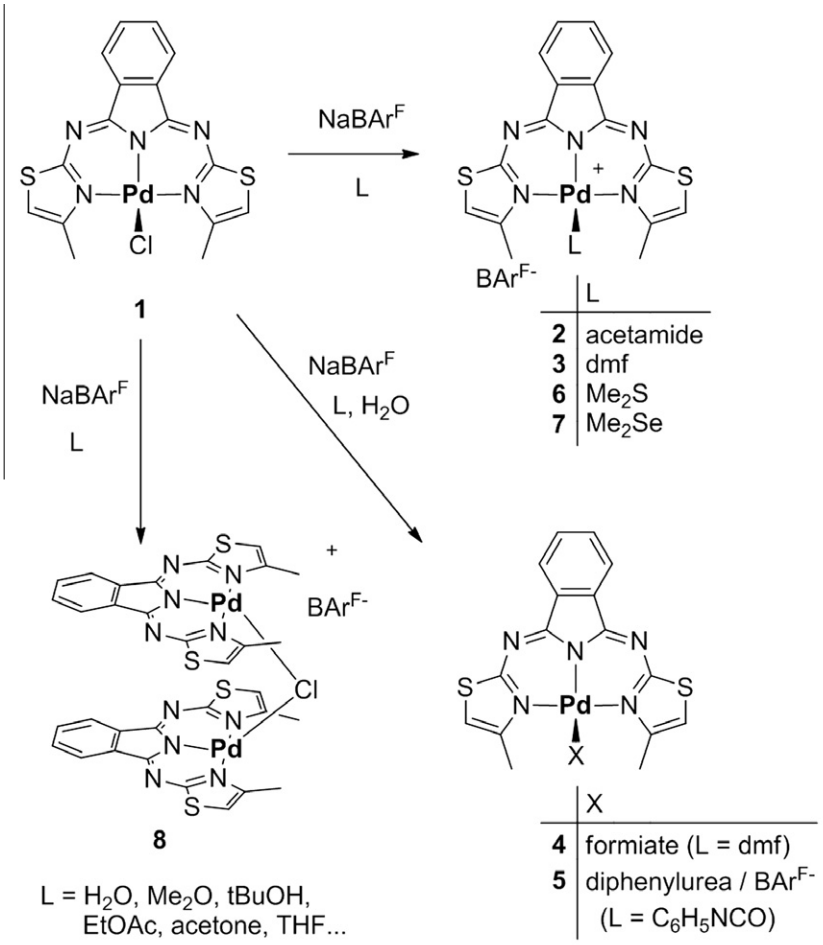

Scheme 1. Overview of ligand exchange reactions performed in this study.

water, alcohols, ketones, aldehydes, esters, and ethers do not form isolable cationic chelate complexes with the (4-Mebti)Pd fragment. Instead, the dinuclear chlorido-bridged species $[\{(4\text{-Mebti})Pd\}_2Cl]^+$ BAr^{F-} **8** [11] forms as the only palladium-containing product during all these attempts. The application of the particularly soft $TeMe_2$ donor on the other side results in the observation of many different reaction products. Obviously, demetalation and decomposition of the organic ligand occurs during the uncontrollable transformation, and a simple $[PdCl(TeMe_2)_3]^+$ complex has been reported as the only isolated species from this mixture [21].

O_{amido}-, S-, and Se-ligands with an intermediate hardness have been found capable to form the desired cationic species. The use of purified acetamide and dmf directly result in the compounds $[(4\text{-Mebti})PdL]^+$ **2** and **3**, respectively, while phenylisocyanate leads to the diphenylurea complex **5** only in the presence of water traces. It is likely that the diphenylurea ligand forms from phenylisocyanate and aniline, which in turn is produced by the hydrolysis of phenylisocyanate. Whether the formation of diphenylurea occurs prior to the metathesis reaction, or is catalyzed by the (4-Mebti)Pd fragment could not be resolved. If freshly distilled phenylisocyanate is used with careful exclusion of water, the dinuclear μ-chlorido derivative **8** forms exclusively. Another hydrolysis product has been obtained from an attempted crystallization of the dmf complex **3** in the presence of wet THF. Several crystals of the neutral formiate species [(4-Mebti)PdOCHO] **4** were isolated as the only product and could be analyzed by X-ray diffraction. As before it is unclear whether the hydrolysis process is catalyzed by the (4-Mebti)Pd fragment or not. A catalytic reaction, however, is quite likely in view of the low tendency of DMF to hydrolyze spontaneously in the presence of water traces [22]. Dimethylsulfide and dimethylselenide react smoothly to the expected products **6** and **7**, respectively. For the selenium derivative, a strict stoichiometric control is necessary in order to avoid the massive formation of by-products from demetalation and ligand decomposition.

All products were obtained in analytical purity after recrystallization, and were characterized by NMR spectroscopy and X-ray diffraction.

3.2. Structural and spectroscopic features

Single crystals have been obtained for the six compounds **2**–**7** by diffusion of *n*-pentane into dichloromethane or dichloromethane/THF (for **4**) solutions at −20 °C. Except for the dmf and urea complexes **3** and **5** all crystals contain co-crystallized dichloromethane or THF molecules (in the case of **4**) to stabilize the crystal lattice. Table 1 contains crystallographic data and details for the structure solutions and refinements. Table 2 summarizes selected molecular data of the investigated complexes.

The acetamide and dmf derivatives **2** and **3**, respectively, crystallize in the triclinic system, space group $P\bar{1}$, with $Z = 2$ (Fig. 2). The palladium(II) ion of **2** is situated in a N_3O ligand field with one short Pd–N bond to the isoindole imido nitrogen donor (1.968(3) Å), two longer Pd–N bonds (2.033(3) and 2.038(3) Å) to the thiazole imino nitrogen donors, and a long Pd–O bond to the acetamide ligand of 2.068(3) Å. The coordination geometry is basically planar with a marked, but evenly distributed distortion

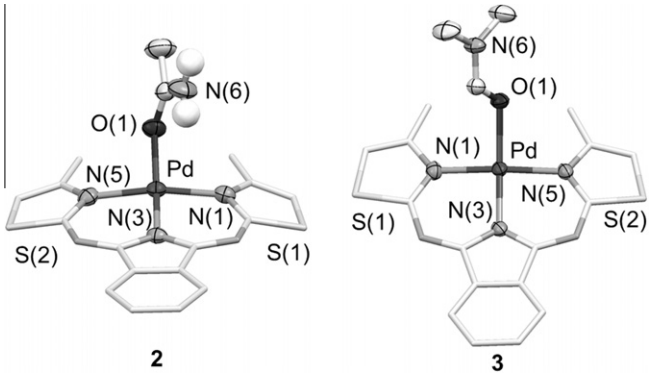

Fig. 2. Molecular structures of acetamide and dmf complexes **2** and **3** (cation only).

towards a tetrahedron. This distortion can be quantified by similar N(1)–Pd–N(5) and N(3)–Pd–O(1) angles of 166.3(1)° and 162.6(1)°, respectively, and accounts for an intermediate amount of steric repulsion between the 4-Mebti ligand and the methyl- and amino groups of the acetamide ligand. The amino group is rotated into conjugation with the carbonyl moiety, and the C–O and C–N bond lengths of the bound acetamide ligand of 1.264(5) Å and 1.295(6) Å, respectively, are clearly aligned as compared to the free acetamide (C–O: 1.242(2)/1.243(2) Å; C–N: 1.325(2)/1.326(2) Å)[23]. This finding accounts for a significant contribution of a resonance structure with a C=N double bond and a partially anionic O-donor, and therefore for an electrophilic activation of the amide functionality in the metal complex. Another noticeable feature of the solid state structure of **2** is the absence of hydrogen bridges between adjacent molecular units. The reason for this observation can be found in the interaction of the complex cation with the BAr^F counterions. The aryl rings of these BAr^F anions are rotated towards each other in a way as to form two juxtaposed *2 phenyl embrace* (2PE) binding pockets [24–28]. One of these pockets binds to the $H_3C–C–NH_2$ motif presented at the surface of the cation and efficiently shields this potent hydrogen bridge donor from interacting with any acceptor site.

The PdN_3O coordination unit of the dmf derivative **3** displays Pd–N bond lengths similar to the acetamide derivative **2** (Pd–N(1): 2.022(3) Å; Pd–N(3): 1.968(2) Å; Pd–N(5): 2.029(3) Å), but differs structurally through the elongated Pd–O(1) bond of 2.100(2) Å. In addition, the non-planar distortion of the PdN_3O unit is unevenly distributed, with a planarized PdN_3 substructure (N(1)–Pd–N(5): 169.59(9)°) and a steep N(3)–Pd–O(1) angle of 156.30(9)°. A possible explanation for these differences lies in the sterical requirements of a significant 2PE binding of the NMe_2 group of the dmf ligand of **3** by a BAr^F anion, which is observed in the crystal structure. Similar to the acetamido ligand of **2**, the NMe_2 group of the dmf ligand of **3** is rotated into conjugation with the binding carbonyl, and the coordination of dmf to the cationic (4-Mebti)Pd fragment again causes an elongation of the C–O bond from 1.2224(6) Å in the free DMF molecule to 1.251(4) Å, and a reduction of the C–N bond length from 1.389(5) to 1.308(4) Å [29]. The polarization of the amide ligand thus appears stronger for dmf than for acetamide. Consequently, the formation of the hydrolyzed formiate complex **4** was observed upon crystallization attempts in the presence of water. The structure of this complex (Fig. 3) resembles largely that of the homologous acetato complex described earlier and will not be discussed in detail [18]. Compared to the cationic amide complexes **2** and **3**, the overall planarized geometry of the PdN_3O subunit of **4** with angles N(3)–Pd–O(2) of 166.7(2)° and 171.8(2)°, and the short Pd–O(2) bond of 2.026(4) Å are the most remarkable features of the neutral formiate complex.

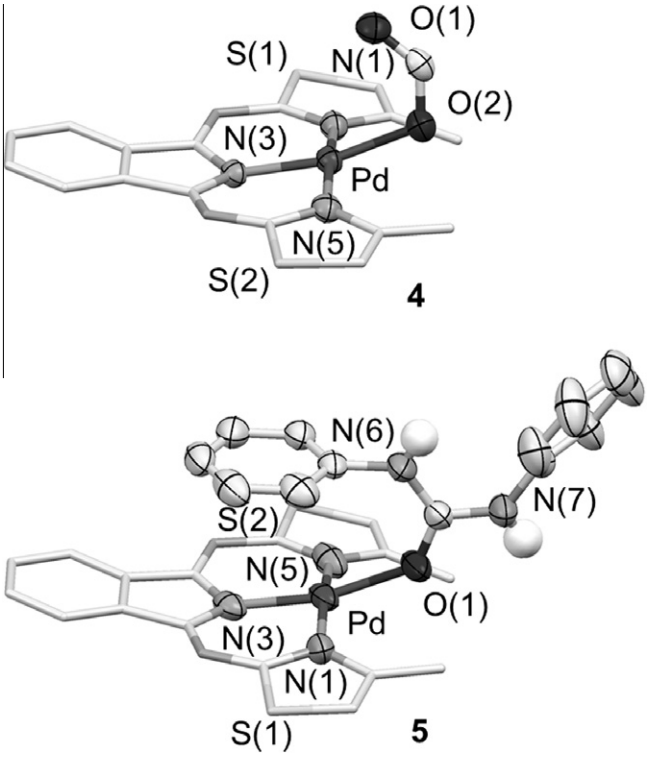

Fig. 3. Molecular structures of formiate and diphenylurea complexes **4** and **5** (cation only).

The second hydrolysis product in this series, the diphenylurea complex **5**, crystallizes in the triclinic system, space group $P\bar{1}$, with $Z = 2$ (Fig. 3). Other than for the other amide derivatives **2** and **3** the bond lengths and angles within the PdN_3O subunit of the urea compound **5** (Pd–N(1): 2.031(4) Å; Pd–N(3): 1.962(3) Å; Pd–N(5): 2.059(4) Å; Pd–O(1): 2.047(3) Å; N(3)–Pd–O(1): 166.2(1)°; N(1)–Pd–N(5): 170.4(1)°) resemble largely those of the neutral formiate **4**. The diphenylurea ligand of **5** contains activated C–O and C–N bonds (C–O: 1.251(4) Å; C–N: 1.327(5) Å and 1.344(5) Å) as judged by the changes found with respect to free diphenylurea (C–O: 1.233(3) Å; C–N: 1.342(5) Å and 1.363(5) Å) [30], albeit the activation appears to be smaller than for the amide ligands in **2** and **3**. A reason for the flattened structure of the PdN_3O coordination unit of **5** may be found in the orientation of the phenyl groups of the urea ligand. While one of these phenyl moieties is bound by the 2PE pocket of the BAr^F anion, the other C_6H_5 unit is π-stacked onto the (4-Mebti)Pd cation with a medium π–π stacking distance of 3.1395(3) Å (distance of the C_6 centroid to the mean squares plane

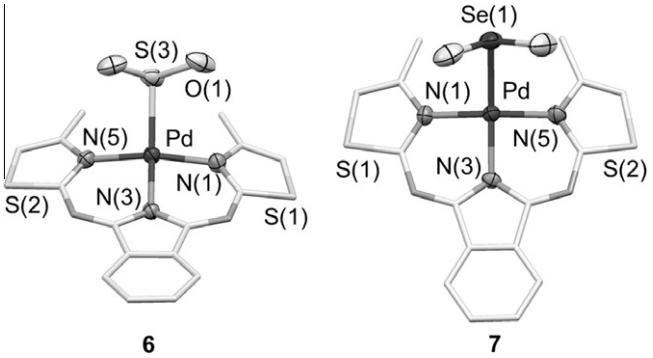

Fig. 4. Molecular structures of dimethylsulfide and dimethylselenide derivatives **6** and **7** (cation only).

Table 3
Correlation of structural parameters and NMR data for the cationic [(4-Mebti)PdL]$^+$ complexes **2**, **3** and **5**–**7**.

Complex (donor ligand)	N(3)–Pd–D (°)	N_{term}–Pd–D (°)[a]	δ[^{1}H] CH_3 (term)
2 (Acetamide)	162.6(1)	92.5	2.57
3 (dmf)	156.30(9)	92.1	2.60
5 (Diphenylurea)	166.2(1)	91.1	2.61
6 (Dimethylsulfide)	151.7(1)	94.8	2.77
7 (Dimethylselenide)	150.8(1)	94.3	2.76

[a] Mean value from N(1)–Pd–D and N(5)–Pd–D.

of all sp^2 atoms of the 4-Mebti ligand, including the Pd atom) and thus tears the whole urea ligand closer to the mean PdN_3 plane.

The EMe_2 complexes (E = S, Se) **6** and **7** crystallize isomorphous in the monoclinic system, space group $P2_1/c$, with $Z = 4$. Fig. 4 illustrates the molecular structures of both [(4-Mebti)Pd(EMe_2)]$^+$ cations. The Pd–E bond lengths in **6** and **7** are found at 2.357(1) Å and 2.4650(8) Å, respectively, and the difference in the bond lengths quantitatively reflects the different vdW radii of the S and Se atom. The C–S–C and Pd–S–C angles at the sulfur atom are 98.3(3)°, 99.4(2)°, and 103.8(2)°, respectively, and therefore slightly larger than the analogous C–Se–C and Pd–Se–C angles of 96.4(4)°, 96.4(2)°, and 101.0(2)°. These values proof the expected decrease of the contribution of the E's *s*-type valence orbital to the binding interaction with increasing atomic number. The geometry of the PdN_3E subunit differs from the amide and urea cases described above by an elongated N(3)–Pd bond of 2.009(3) Å (E = S) and 2.010(4) Å (E = Se), and by significantly larger N(3)–Pd–E angles of 151.7(1)° (E = S) and 150.8(1)° (E = Se). Beside the obviously larger vdW radii of S and Se, the fact that the orientation of these two EMe_2 ligands is perpendicular to those of the O-donor ligands in **2**–**5** accounts for an additional gain in L···4-Mebti repulsion, and thus in a higher degree of distortion.

The structurally characterized cations of **2**, **3**, **5**, **6**, and **7** can be divided roughly into two groups by the degree of distortion of the PdN_3D subunits in the crystal lattice. The first group contains the amide and urea ligands with soft O-donors carrying a partial negative charge due to efficient conjugation with adjacent amino groups. This group is characterized by an intermediate distortion, and the exception of the urea compound **5** can easily be rationalized by the presence of additional π-stacking interactions. The second group consists of the EMe_2 derivatives (E = S, Se), for which a large distortion has been found. This interpretation is further supported by the ^{1}H chemical shift of the terminal methyl group protons in solution (Table 3). A clear correlation has been observed with high field signals for the first group and low field signals for the second. Other than in the solid, the urea species **5** fits well into the first group in solution. A similar correlation has been found before for a series of cationic palladium tripyrrins [8] and thus seems to provide a simple, general probe for future studies in this field.

4. Conclusions

Soft O_{amide}-, S-, and Se-donor ligands bind well to the cationic (4-Mebti)Pd fragment and allow for a number of crystallographically characterized distorted complexes of the pseudo-planar geometry. As for the related palladium tripyrrin complexes with group 14 and 15 donor ligands, the degree of distortion depends mainly on the sterical requirements of the employed ligands, and can be monitored in solution by the shift of the ^{1}H NMR signal of the terminal methyl group protons. Harder O-donor ligands, on the other hand, cannot compete with the binding strength of the bridging chlorido ligand of a dinuclear μ-chlorido complex, which appears to be the common intermediate in all ligand exchange reactions studied here. This result fits into the general expectations from the HSAB concept and shows, that besides the sterical component, the ligand softness must be considered in future attempts to prepare three-coordinate palladium(II) complexes.

Acknowledgements

Funding was kindly provided by the Deutsche Forschungsgemeinschaft (DFG). The authors thank Nicola Biermann for his help with the dmf derivative **3**.

Appendix A. Supplementary material

CCDC Nos. 813871 (**2**), 813872 (**3**), 813870 (**4**), 813867 (**5**), 813869 (**6**), and 813868 (**7**) contain the supplementary crystallographic data for this paper. These data can be obtained free of charge from The Cambridge Crystallographic Data Centre via http://www.ccdc.cam.ac.uk/data_request/cif. Supplementary data associated with this article can be found, in the online version, at doi:10.1016/j.ica.2011.02.080.

References

[1] R. van Eldik, Coord. Chem. Rev. 182 (1999) 373.
[2] M. Bröring, C.D. Brandt, Chem. Commun. (2001) 499.
[3] M. Bröring, C.D. Brandt, S. Prikhodovski, J. Porphyrins Phthalocyanines 7 (2003) 17.
[4] M. Bröring, C.D. Brandt, J. Chem. Soc., Dalton Trans. (2002) 1391.
[5] M. Bröring, S. Prikhodovski, C.D. Brandt, E. Tejero, Z. Anorg. Allg. Chem. 633 (2007) 458.
[6] M. Bröring, C.D. Brandt, Chem. Commun. (2003) 2156.
[7] M. Bröring, C.D. Brandt, S. Stellwag, Chem. Commun. (2003) 2344.
[8] M. Bröring, C.D. Brandt, S. Link, Inorg. Chim. Acta 358 (2005) 3122.
[9] M. Bröring, C. Kleeberg, Inorg. Chim. Acta 360 (2007) 3281.
[10] M. Bröring, C. Kleeberg, J. Porphyrins Phthalocyanines 12 (2008) 839.
[11] M. Bröring, C. Kleeberg, Z. Anorg. Allg. Chem. 634 (2008) 2793.
[12] M. Brookhart, B. Grant, A.F. Volpe Jr., Organometallics 11 (1992) 3920.
[13] L. Syper, J. Mlochowski, Synthesis (1984) 439.
[14] G.M. Sheldrick, Acta Crystallogr. A64 (2008) 112.
[15] A. Altomare, G. Cascarano, C. Giacovazzo, A. Gualardi, J. Appl. Crystallogr. 26 (1993) 343.
[16] A.L. Spek, PLATON, A Multipurpose Crystallographic Tool, Utrecht University, The Netherlands, 1998.
[17] L.J. Farrugia, J. Appl. Crystallogr. 32 (1999) 837.
[18] M. Bröring, C. Kleeberg, Z. Anorg. Allg. Chem. 633 (2007) 2210.
[19] P.-G. Lassahn, V. Lozan, C. Janiak, Dalton Trans. (2003) 4437.
[20] F. Blank, C. Janiak, Coord. Chem. Rev. 253 (2009) 827.
[21] M. Bröring, C. Kleeberg, Z. Anorg. Allg. Chem. 634 (2008) 946.
[22] R.A. Fersht, Y. Requena, J. Am. Chem. Soc. 93 (1971) 3499.
[23] J.W. Bats, M.C. Haberecht, M. Wagner, Acta Crystallogr. E 59 (2003) o1483.
[24] C.A. Hunter, Chem. Soc. Rev. 23 (1994) 101.
[25] C. Janiak, J. Chem. Soc., Dalton Trans. (2000) 3885.
[26] M. Scudder, I. Dance, J. Chem. Soc., Dalton Trans. (1998) 3167.
[27] I. Dance, M. Scudder, J. Chem. Soc., Dalton Trans. (2000) 1587.
[28] V. Russel, M. Scudder, I. Dance, J. Chem. Soc., Dalton Trans. (2001) 789.
[29] G. Schultz, I. Hargittai, J. Phys. Chem. 97 (1993) 4966.
[30] Rajnikant, Dinesh, M.B. Deshmukh, Kamni, Bull. Mater. Sci. 29 (2006) 239.